Applied Radiation and Isotopes 236 (2026) 112764

Contents lists available at ScienceDirect

Applied Radiation and Isotopes

journal homepage: www.elsevier.com/locate/apradiso

A novel method of gamma ray emission estimation to assess fuel burnup in reactor systems with continuous fuel circulation

Justin Shurie, Ben Impson, Zeyun Wu, Braden Goddard *

Department of Mechanical and Nuclear Engineering, Virginia Commonwealth University, 401 West Main Street, Richmond, VA, 23284-3068, USA

ARTICLE INFO

Keywords:
Monte Carlo
HPGe
Pebble bed reactor
Molten salt reactor
Burnup
Gamma spectroscopy
Nuclear fuel

ABSTRACT

Accurate characterization of gamma-ray signatures from advanced reactors with mobile fuels, such as Pebble Bed Reactor (PBRs) and Molten Salt Reactor (MSRs), remains challenging due to continuously varying fuel locations, compositions, and irradiation histories. This work presents a Monte Carlo-based framework for generating high-fidelity synthetic gamma spectra corresponding to known fuel conditions and burnup states using coupled radionuclide inventory calculations and High-Purity Germanium (HPGe) detector modeling. The methodology models individual gamma-emitting radionuclides separately using characteristic emission energies and branching intensities, while accounting for self-attenuation and transport through fuel and surrounding materials. Detector responses are calculated using MCNP simulations and subsequently combined using radionuclide-specific activities and emission yields to produce composite spectra where gamma intensity is represented in counts per second. The objective of this work is not to directly determine burnup from measured spectra, but rather to establish a physics-based spectral generation capability that can support future development, calibration, and evaluation of burnup monitoring techniques for mobile-fuel reactor systems. The framework allows systematic variation of reactor, fuel, and detector parameters to evaluate spectral sensitivity to changing fuel conditions and operating states. This approach provides a foundation for safeguards, diagnostics, and future nondestructive assay methodologies in advanced reactor technologies.

1. Introduction

Advanced reactor designs, such as Pebble Bed Reactors (PBRs) and Molten Salt Reactors (MSRs) have been developed with distinct refueling strategies intended to reduce or eliminate the need for periodic refueling and the downtime that accompanies it. Most PBRs consist of packed beds of spherical, fuel-containing graphite pebbles (Claxton, 1966), such as X-energy's Xe-100 reactor (Carter et al., 2022), which employs TRISO-X pebble fuel (Loza). In these systems, fresh or recirculated pebbles are introduced at the top of the reactor while pebbles are removed from the bottom, resulting in a gradual downward movement of fuel through the core. MSRs, in contrast, generally fall into two main categories: one that employs static fuel elements in which molten salt serves only as the coolant, and another in which the nuclear fuel is dissolved into the molten salt, allowing the salt to function simultaneously as fuel and coolant as it circulates through the reactor system (Serp et al., 2014; Status of Molten Salt Reactor, 2023). In both PBRs and MSRs with circulating or otherwise mobile fuel, determining the number of fissions per unit mass of fuel – commonly referred to as burnup – poses additional challenges (Kovacic et al., 2018, 2023) compared with static-fueled systems and more conventional reactor designs such as pressurized water reactors (PWR) and boiling water reactors (BWR) (Kovacic et al., 2018, 2023).

Burnup calculation or measurement is an integral part of the nuclear fuel management process, as it determines which fuel elements are discharged from the core, which are repositioned, and where fresh fuel is inserted (Turinsky et al., 2005; Zafar et al., 2019). Burnup estimation and fuel management are considered simpler in reactors with static fuel because fuel positions are fixed and well known. By combining the reactor's operational history with local neutron flux distribution, reasonably accurate burnup estimates can be obtained. However, in reactors with mobile fuels like PBRs and MSRs, the absence of a well-defined fuel trajectory through the core significantly complicates burnup determination. In PBRs, it also becomes difficult to distinguish between individual fuel elements, while in MSRs the fuel behaves as a largely homogenous mixture due to continuous circulation and mixing.

As a result, mobile-fueled reactors such as MSRs and PBRs must either undergo periodic full refueling because fuel cannot be shuffled

* Corresponding author.
E-mail address: bgoddard@vcu.edu (B. Goddard).

https://doi.org/10.1016/j.apradiso.2026.112764
Received 10 April 2026; Received in revised form 26 May 2026; Accepted 17 June 2026
Available online 19 June 2026

based on burnup, or must implement a refueling strategy that selectively removes high-burnup fuel and replaces it with fresh or low-burnup fuel, known as online refueling. The first option is undesirable because, compared with static-fueled reactors, it results in poorer fuel utilization and more frequent downtime. Online refueling, in contrast, leverages the mobility of the fuel to assess the burnup of individual fuel elements (in PBRs) or of the circulating fuel inventory (in MSRs). However, because fuel elements cannot be readily distinguished and their prior trajectories through the core are unknown, burnup determination relies primarily on non-destructive assay (NDA), which is the process of determining the fuel composition without damaging the fuel or removing physical samples (Reinovsky and Favalli, 2019; Bolzonella, 2023).

Historically, NDA of used nuclear fuel has relied on several approaches, with gamma-ray spectroscopy being particularly valuable because it enables the identification and quantification of specific radionuclides (Dragnev, 1973). This approach typically focuses on key gamma emitters such as ^{137}Cs, ^{134}Cs, and ^{154}Eu (Willman et al., 2006). These fission products possess at least one prominent gamma emission with high emission probability and energies above the 94-111 keV uranium K-shell x-rays. They also have half-lives on the order of years and relatively high cumulative fission yields from both uranium and plutonium (Geist et al., 2024). These characteristics make them well suited for burnup estimation through measurement of their gamma-ray peaks and determination of their respective inventories. By using the activities or masses of these radionuclides, along with their isotopic ratios, gamma spectroscopy - focused on ^{137}Cs, ^{134}Cs, and ^{154}Eu - has been used to estimate burnup in fuel discharged from both PWRs (Caruso et al., 2007) and PBRs (Mulyana and Chirayath, 2024), in addition to other reactor types. For PWR fuel, reported burnup estimates showed errors of approximately 2% at low burnup, increasing to as much as 23% at higher burnup levels (Caruso et al., 2007). Errors of this magnitude can lead to fuel underutilization, degraded reactor performance, or even cause a safety issue. Consequently, the three conventional indicators - ^{137}Cs, ^{134}Cs, and ^{154}Eu - can be supplemented by monitoring short-lived radionuclides (Lakosi and Veres, 1990). This approach is feasible in systems where measurements are performed on fuel that was in the reactor core only seconds earlier, rather than after extended cooling following discharge.

Online fuel burnup characterization of PBR and MSR fuel consists of two primary stages. The first stage is the measurement of gamma emissions from the fuel sample. Ideally a continuous process, the exact implementation of this can differ between designs. One implementation is that of a constantly moving fuel; PBR pebbles that roll towards and then away from a detector, or a constant stream of MSR fuel salt. Another possible implementation is a staged flow; pebbles are stopped in front of the detector before being moved away, or molten salt is held in a small vessel that fills and empties cyclically. The second stage of online burnup characterization involves data analysis, where the measured gamma spectrum is used to determine the burnup of the fuel element.

A necessary precursor to this second stage of burnup characterization is the ability to accurately predict detector response from known radionuclide inventories under realistic fuel and detector conditions. The present work focuses specifically on this forward modeling problem by generating synthetic gamma spectra for fuel compositions at different burnup levels in two advanced reactor systems.

2. Detector measurement

Gamma-ray detection was simulated by modeling of a fuel pebble and a salt sphere 4 cm away from a typical coaxial P-type High-Purity Germanium detector (HPGe)(Snook, 2024; Snook et al., 2026). All photons entering the live portion of the detection crystal were recorded as tallies in their respective energy bins. In the case of the pebble, gamma rays are generated in the fuel region of the pebble, not the individual TRISOs. This would have a minor impact on attenuation; however, this inaccuracy does not significantly affect the work. Because the gamma ray generation sites and directions are randomly selected, there is a strong probability that gamma rays will traverse at least one TRISO particle while transiting the pebble. Fig. 1 shows an example plot generated from a pebble with TRISOs present in comparison to a dummy pebble without any TRISO particles present (only the graphite matrix). Three peaks, due to gamma induced X-rays in the uranium, are present in the spectrum measured with TRISOS that are not present in the spectrum without TRISOs. This demonstrates that the gamma rays are interacting with and are attenuated by the TRISO particles, despite being generated randomly within the fuel region.

For the MSR fuel salt, the same detector model and experimental setup were used, with the fuel pebble being replaced with fuel salt. The salt was modeled as a sphere above the detector and contained the nuclides present after varying levels of burnup and cooling. The choice to model the salt as a static sphere with dimensions equal to that of a pebble is to allow a direct comparison between the two fuel forms. In reality, the molten salt can be measured in different geometric and material forms. The same process of measuring the individual gammas of each gamma emitter was performed using the salt model. As the salt is a homogeneous mixture, the specific concern regarding gamma attenuation present for the heterogeneous pebble model was absent from the salt model.

To obtain the tally data used in this study, each gamma-emitting radionuclide was simulated independently using the code Monte Carlo N-Particle 6.2 (Werner et al., 2018) (MCNP) running in photon mode (p mode). A verification test was conducted first, running simulations in coupled photon-electron transport model (p-e mode), which showed no statistically significant differences compared with simulations performed solely in p mode. Each gamma emission was assigned an intensity based on evaluated nuclear data (From ENSDF database as of, 2024; International Atomic Energy Agency (IAEA and), 2024). Gamma emissions predicted by nuclear data but not experimentally observed were not included. All MCNP simulations were performed using one billion particle histories per radionuclide to ensure adequate statistical convergence and consistency among all radionuclides. The HPGe detector employed 16,384 energy bins with a resolution of 0.5 keV per bin, resulting in an upper energy limit of 8.192 MeV. For each independent radionuclide run to produce tally data, the average mass of every nuclide across all burnup steps was used to provide attenuation.

3. Analytic data processing

The tallies produced by MCNP are not inherently useful in themselves. While they provide insight into the effect attenuation will have on gamma measurements, this could just as easily be calculated by hand. However, they provide a baseline that can be used to develop a method of scaling the gammas to the mass present in the pebble.

The tallies from MCNP are in units of counts per gamma. They would be much more useable if they were in counts per gram per second. That conversion process is fairly straightforward; however, exact values will depend on the radionuclide in question. Fig. 2 illustrates a baseline of the data processing procedure.

This process requires several inputs to be useable. First, it requires a baseline gamma ray measurement based on individual radionuclides. That measurement needs to be scaled by the mass, which is the other input. This means, to be field useable as a point of comparison, a radiation transport model of whatever material is being measured should be used to develop a baseline for potential gamma ray emissions. This baseline can then be used to determine what gammas could be expected at a given step in a burn cycle.

The calculation methodology and associated data were implemented in a Microsoft Excel spreadsheet. The user inputs the ZAID identifier (atomic and mass identification number) and corresponding mass for each radionuclide present in the sample. If a different MCNP model is used, the tally counts for each gamma-emitting radionuclide must be

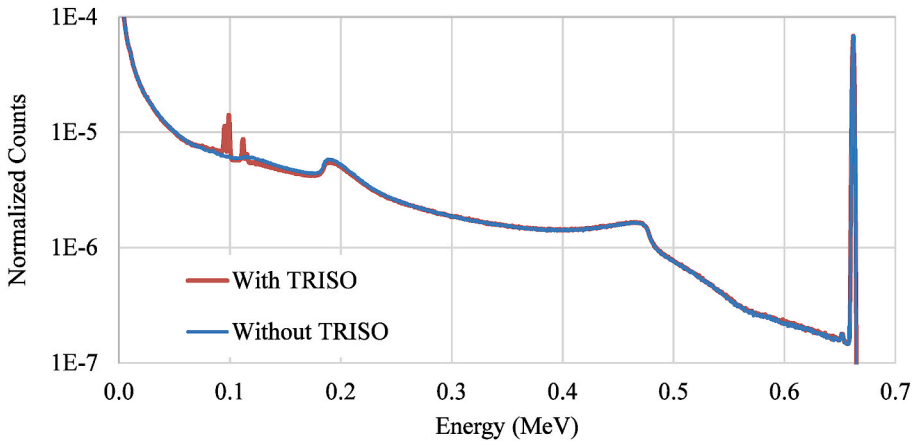

Fig. 1. Detector response from a 662 keV gamma-rays source with and without TRISO particles present.

Fig. 2. Process for unit conversion from counts per gamma to counts per second.

updated accordingly.

Using the radionuclide intensity, specific activity, and mass, the spreadsheet converts the MCNP tally output from counts per gamma emission to counts per second. The intensity and specific activity are constant for a given radionuclide, while the radionuclide mass is treated as an input variable. The resulting spectra can then be plotted using either energy values or bin numbers along the horizontal axis. These plots represent the simulated gamma-ray interactions within the active region of the HPGe detector under the specified MCNP tally conditions.

The methodology is applicable to tally data generated from any MCNP model and for any energy range. In the present work, an energy range from 0 to 8192 keV with 0.5 keV bin widths was used to capture all significant gamma-ray emissions.

4. Discussion of pebble bed reactor applications

4.1. Pebble model

The fuel pebble model used for this work was developed in our earlier work studying the effect of particle position randomization on the neutron spectrum (Impson et al., 2025), also using MCNP 6.2. It is a single fuel pebble, in a cube of helium with reflective boundaries and contains discrete, randomized TRISO particles. This represents, in effect, a fuel pebble at the center of the reactor for the entirety of its burn cycle. For the inventory, this pebble was burned for 1304 days to 160 GWd/MTU (Carter et al., 2022; Loza; Impson et al., 2025). The MCNP burnup simulation includes 30 days of cooling time, modeled as burnup with 0 power. The radionuclide list for gamma ray measurements is taken from the end of the burn cycle. This allows for the possibility of short-lived radionuclides to be measured for their gammas, but they may or may not appear in the mass inventory depending on the time of the gamma measurement. Pebbles are expected to cycle multiple times and could be measured at any of these times. The gamma emitters present at each time will vary considerably. The radionuclides present will also depend on the path through the reactor core. Although this model represents an average center path pebble, work is currently being conducted at Virginia Commonwealth University on a full reactor model with distinct pebble regions (Mehta et al., 2024).

4.2. Pebbles at different burnup times

Several assumptions should be made when estimating the gamma rays and masses present in fuel pebbles (the only type of pebble that will be discussed from here on). For simplicity's sake, it is assumed that the gamma rays emitted by the pebbles are measured at 6 time steps between their initial insertion and their final removal. This aligns with the estimated 6-7 cycles through an operating reactor. Second, assume negligible cooling time between cycles, as even if a pebble spends a day or two out of the core, it will be promptly measured and once reinserted, will quickly build up the lost short-lived fission products to equilibrium. Third, assume the time between each measurement is approximately one sixth of the total burn time. For this model, there were 1304 days of burnup such that a measurement is modeled approximately every 220 days following insertion. The discussion of the gamma spectra for the burned pebble focused on the range between 500 keV and 1 MeV, because many short-lived burnup-determining radionuclides produce gamma rays in this range.

All loaded fuel pebbles initially contain fresh fuel, with no fission products or actinides besides uranium. Each uranium isotope emits gamma rays, although they are of low activity. Fig. 3 shows the gamma rays spectrum from a fresh fueled pebble, with the uranium of the UCO fuel kernel enriched to 15.65 wt%. As can be seen, the peaks expected from an enriched uranium sample are present. Most notable is the peak at 185.72 keV, a predominant ^{235}U gamma ray (Gawad et al., 2019). ^{235}U gammas are more prominent than the ^{238}U gammas, due to the much higher specific activity of ^{235}U. ^{238}U's gamma rays at 49.55 keV and 113.5 keV are not discernible, with the 49.55 keV ray not registering any counts due to absorption, the 113.5 keV gamma ray contributes only 0.5391% of the total gamma intensity in the 113.5 keV energy bin. Gamma emitting decay products such as ^{226}Ra and ^{234m}Pa were not included, as the simplified model assumed no prior decay had occurred before irradiation, and at no point did either constitute above 10^{-10} atom fraction of the UCO fuel, the default MCNP burnup cutoff.

Once 218 days have passed (26.7 GWd/MTU), fission and decay gamma emitters are present in the pebble, as can be seen in Fig. 4. At this low burnup, there has been minimal production of radionuclides typically used as burnup indicators. ^{137}Cs for example, is present at 717.8 keV, but is overshadowed by ^{143}Ce at 721.9 keV and ^{95}Zr at 724.2 keV. This initial increase in counts in the 0.5 MeV to 1.0 MeV region is due to ^{135}I and ^{140}La, contributing 38.4% and 33.2% of the

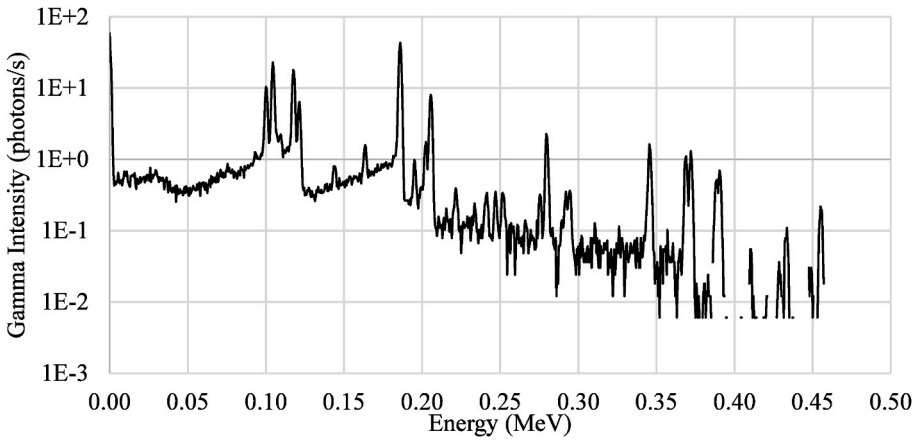

Fig. 3. HPGe gamma spectrum of a pebble with fresh fuel for the 0 keV to 500 keV range.

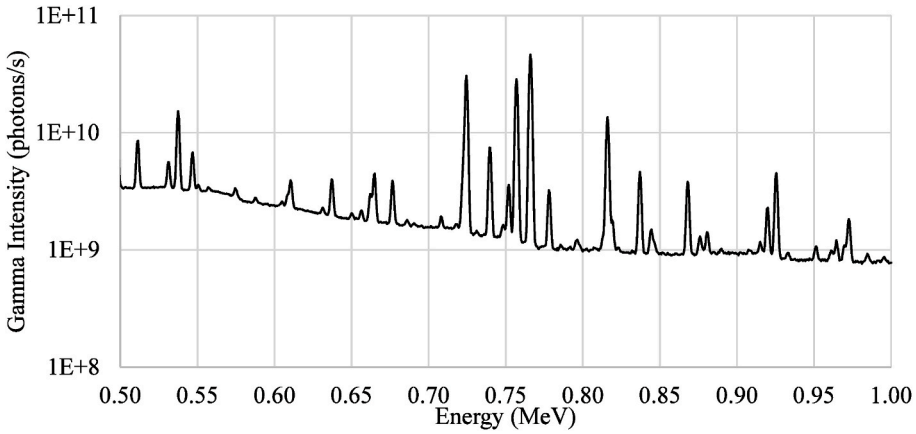

Fig. 4. HPGe gamma spectrum of a pebble burned 218 days with burnup at 26.7 GWd/MTU.

total counts across these bins, on average. The half-life of these two elements are 6.58 h for ^{135}I and 1.67858 days for ^{140}La. As such, they are expected to be relatively consistent across all stages of burnup, and to diminish quickly once production stops. ^{140}La is produced by beta decay of ^{140}Ba with a half-life of 12.751 days, such that production will not sharply decrease with cooling time. ^{135}I however is produced both by fission and by beta decay of ^{135}Te, with a half-life of 19 s, so production is expected to stop within minutes of the fuel leaving the reactor.

The spectrum after 458 days in the reactor (56.2 GWd/MTU) can be seen in Fig. 5. Most peaks are approximately the same height compared to the prior measurement, with only a slight increase in overall intensity, with a few notable exceptions. These exceptions are due to ^{134}Cs, ^{136}Cs, ^{137}Cs and ^{238}Np. The two peak changes due to ^{134}Cs are at 604.721 keV and 795.864 keV, corresponding to decay gammas with absolute intensities of 97.62% and 85.46% respectively. The ^{137}Cs peak at 661.657 keV also becomes more prominent between these measurements when compared to its neighboring peak at 664.571 keV due to ^{143}Ce. ^{134}Cs and ^{137}Cs are conventional burnup indicators, however there are two additional changes of note between the spectra at 26.7 and 56.2 GWd/MTU. ^{136}Cs has a decay gamma with an absolute intensity of

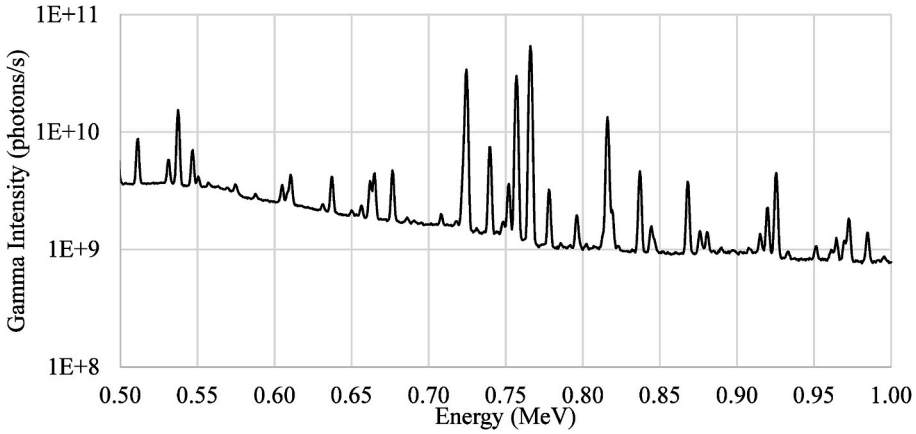

Fig. 5. HPGe gamma spectrum of a pebble burned 458 days with burnup at 56.2 GWd/MTU.

99.7% at 818.514 keV, and ^{238}Np has a decay gamma of absolute intensity 25.2% at 984.45 keV.

The gamma spectrum following the third cycle is shown in Fig. 6, after 698 total days in the reactor (85.6 GWd/MTU). Similar to the comparison between the prior two measurements, most peaks present at 458 days are the same height at 698 days, again with exceptions. At ~744 keV, the spectra after 458 days of burnup was flat, but at 698 days a peak exists, due to ^{244}Am which contributes 24.33% of the total gamma intensity of the bin, compared to the mere 5.125% of the total gamma intensity it contributed at 458 days. ^{244}Am has two visible decay peaks in this spectrum, the first at 743.971 keV with an intensity of 66%, and the second at 897.848 keV with intensity 28%. This second peak was already visible, but in both timesteps, ^{148}Pm has a decay gamma of 896.42 keV which contributes approximately 5% of the total intensity of the bin despite only having a decay intensity of 0.981%. Production of ^{148}Pm also increases over time despite the short half-life, only 5.368 days, as ^{147}Pm builds up in quantity, with half-life of 2.6234 years, creating ^{148}Pm by (n,γ) reaction.

Other notable changes are the increased areas of the ^{134}Cs peaks at 604.721 keV and 795.864 keV with decay intensities of 97.62% and 85.46% respectively, while three new peaks at 563.246 keV, 569.331 keV and 801.953 keV are also due to ^{134}Cs, with decay intensities of 8.338%, 15.373% and 8.688% respectively. Finally, the peaks from ^{136}Cs at 818.514 keV, and from ^{238}Np at 984.45 keV have once again increased in area.

On the fourth cycle after 938 total days (115.1 GWd/MTU), shown in Fig. 7, the most drastic change to the graph is the sharp increases of the peaks at 743.971 keV and 897.848 keV caused by ^{244}Am being 325.5% of its concentration at 698 days of burnup. The half-life of ^{244}Am is only 10.1 h, and while cooling time between irradiation steps is not simulated in the initial burnup model, actual pebble circulation outside of the active core is not expected to last hours, making ^{244}Am a decent indicator of how long a sample has been at power without significant outages or power reduction. The more conventional indicators also show increased quantities, with increases in the five already distinct peaks of ^{134}Cs. Further, ^{137}Cs and ^{136}Cs are present in increased quantity evidenced by their increased peaks at 661.657 keV and 818.514 keV respectively. The increase in ^{238}Np from 698 days to 938 days is by a factor of 186.0%, reflected in increases in the increase of the 984.45 keV peak it emits.

Fig. 8 shows the next step, 1138 days into the burnup (139.6 GWd/MTU). No new peaks emerge, with continual increases of ^{134}Cs (563.25 keV, 569.33 keV, 604.72 keV, 795.86 keV and 801.95 keV), ^{137}Cs (661.66 keV), ^{244}Am (743.97 keV and 897.85 keV), ^{136}Cs (818.514 keV) and ^{238}Np (984.45 keV). Notably there are decreases in 757 keV and 766 keV, the third tallest and tallest peaks respectively.

At 756.725 keV, ^{95}Zr emits gamma radiation at 54.38% intensity, as well as 724.192 keV at 44.27% intensity. The mass of ^{95}Zr peaks at 458 days of burnup, resulting in the decrease of the peak near 757 keV, however no decrease is observed near 725 keV due to increasing concentrations of ^{105}Ru emitting decay gamma radiation at 724.211 keV with intensity 47.8%. At 764.803 keV, ^{95}Nb emits decay gamma radiation at 99.808% intensity. The mass of ^{95}Nb also peaks at 458 days of burnup.

At 1304 days (160 GWd/MTU), the pebble is permanently removed from the reactor core. This is represented in the MCNP model by reducing the power output to 0 MW. Shown in Fig. 9, the gamma spectrum from this final power step illustrates the same trend seen in recent figures, with increases in peaks caused by ^{134}Cs, ^{137}Cs, ^{244}Am, ^{136}Cs and ^{238}Np, and decreases in two of the most prevalent peaks, those due to ^{95}Zr and ^{95}Nb. Only one of the two ^{95}Zr peaks is seen to decrease as the other is compensated for by an overlapping ^{105}Ru peak.

While it remains unclear how long a pebble will be cooled before disposal, it is generally expected to be between 6 h and ten days (Gawad et al., 2019). Taking a measurement approximately in the center of that span, five days, would produce Fig. 10. This figure was generated by following the 1304 day, 160 GWd/MTU with 7 burnup steps at zero power totaling 5 days of additional cooling and comparing it to the data from the fuel composition prior to this cooling. Five days is enough for short-lived fission products and actinides to decay, decluttering the spectrum considerably. The 661.66 keV peak produced by ^{137}Cs is distinct, without interference from other gamma emitters, namely ^{143}Ce at 664.571 keV. The strongest gamma rays from ^{134}Cs, 604.72 keV and 795.86 keV are also easily identifiable. The peaks from ^{134}Cs and ^{137}Cs can be used to calculate the overall burnup of the reactor, using known data about the reactor power (Kovacic et al., 2023). The ratio "r" of ^{134}Cs to ^{137}Cs when compared to burnup "B" in GWd/MTU reveals a fit of $B = 1316r - 2.79$, with $R^2 = 0.9985$.

Much of the usefulness of this method would depend on relative data. It is expected that a portion of the initial pebbles that run through a reactor will be disassembled for analysis. By sampling pebbles at different points in the cycle, the relative buildup of radionuclides in the average pebble can show the approximate burnup. This could also be done through simulations. Work is being conducted in several places that would allow for burnup analysis of a full reactor core (Mehta et al., 2024; Suparlina and Setiadipura, 2019; Dim et al., 2023). These works group the pebbles into smaller sections of the reactor. Through this work, an approximate radionuclide inventory of different regions and paths through the reactor can be developed.

In conclusion, by observing the burnup progression of a PBR pebble, usage of the ratio between ^{134}Cs to ^{137}Cs is appropriate in determining pebble burnup. It should be noted however, that ^{137}Cs only has a gamma ray at 661.657 keV at 85.1% intensity, which can be partially obscured by ^{143}Ce if measurements are taken shortly after the pebble is taken out

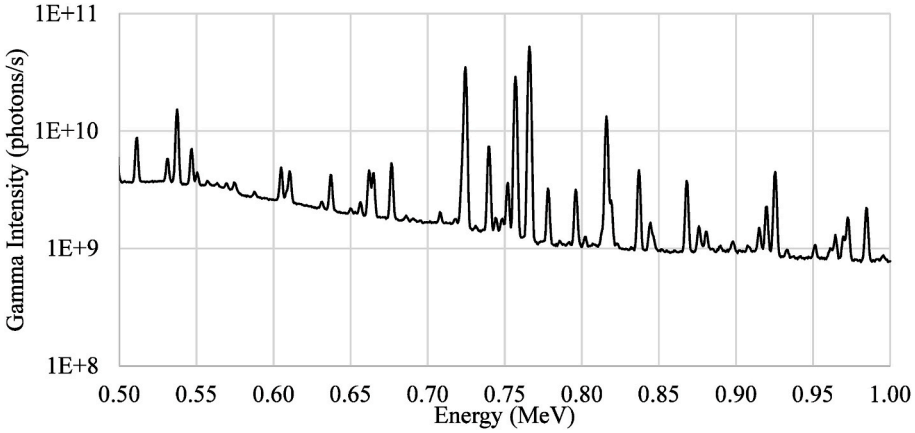

Fig. 6. HPGe gamma spectrum of a pebble burned 698 days with burnup at 85.6 GWd/MTU.

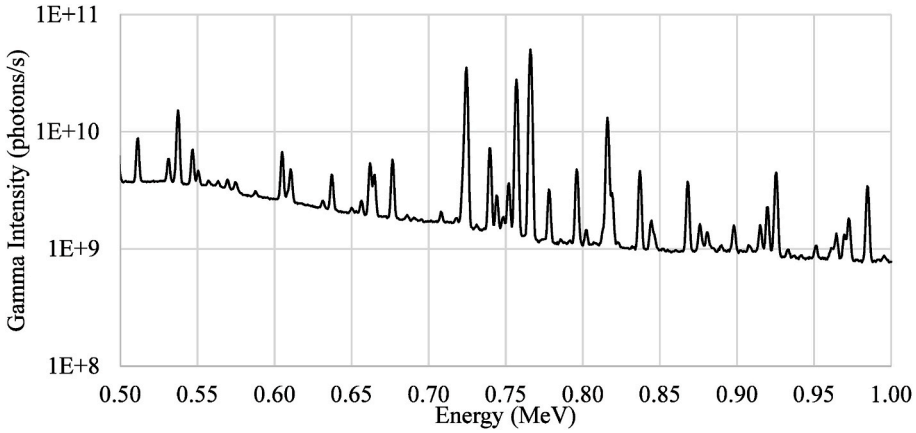

Fig. 7. HPGe gamma spectrum of a pebble burned 938 days with burnup at 115.1 GWd/MTU.

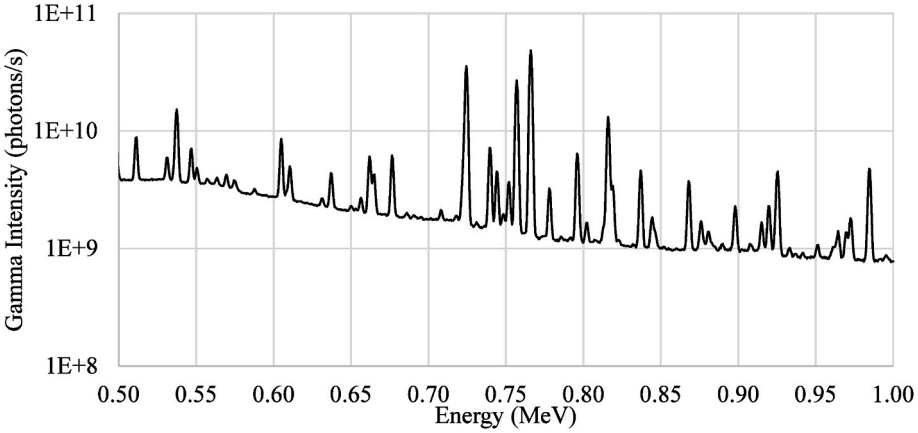

Fig. 8. HPGe gamma spectrum of pebble burned 1138 days with burnup at 139.6 GWd/MTU.

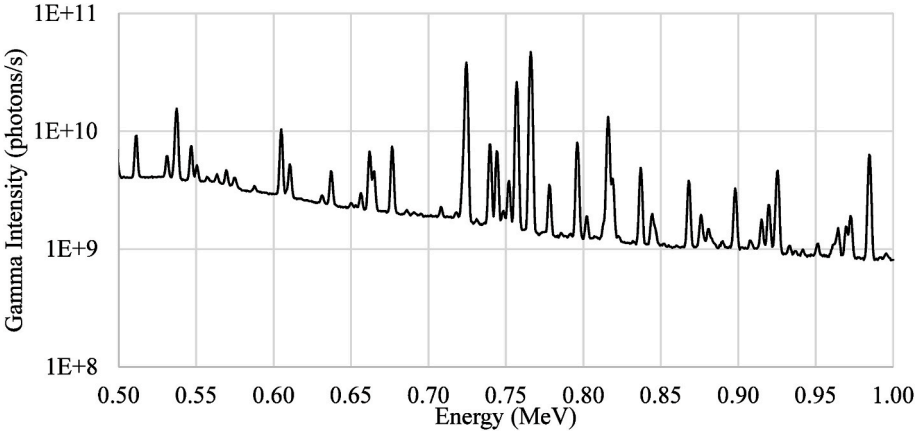

Fig. 9. HPGe gamma spectrum of a pebble burned 1304 days with burnup at 160 GWd/MTU.

of the reactor. This tool may be beneficial to help isolate this peak by removing ^{143}Ce. Using a measured spectrum, the peaks of ^{143}Ce can be accounted for by calculating the mass of ^{143}Ce present using the 587.20 keV peak it emits with intensity of 0.267% and applying this mass to account for its contributions to the total gamma spectra caused by its 664.571 keV peak, emitted at an intensity of 5.69%.

5. Discussion of molten salt reactor applications

5.1. Molten salt model

The MSR model that is studied here is adopted from U-tube Stationary Salt Reactor (USSR) model of our earlier work (Shurie et al., 2024), which is designed to burn actinides present in used light water reactor (LWR) fuel. The entire USSR core is modeled with non-reflective boundaries surrounding the reactor vessel's exterior. While considered a

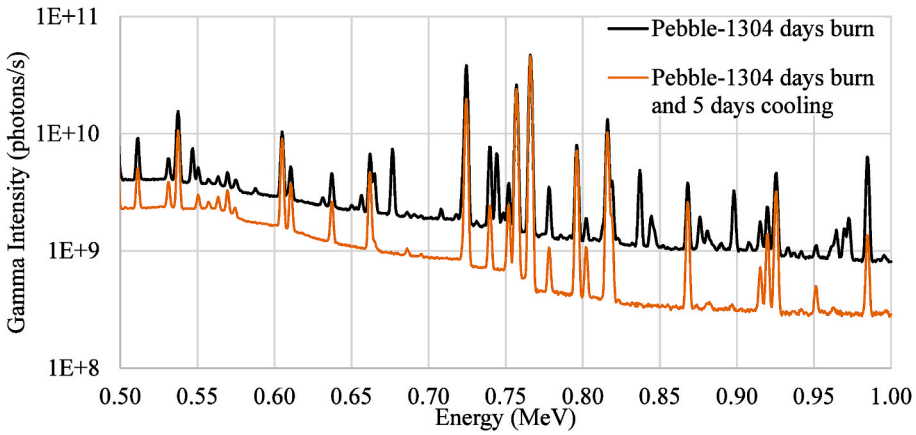

Fig. 10. HPGe gamma spectrum of a pebble with burnup at 160 GWd/MTU with and without 5 days of cooling.

stationary salt reactor, the molten fuel salt still experiences intermixing, so a homogenous fuel composition is used throughout the core during burnup calculation. The computational model used does not account for the online refueling process planned to take place, nor does it account for the automatic removal of fission gases. As such, the burnup experienced within the USSR model is unrefined but is still included for comparison.

Online refueling is planned for the USSR, but real-time determination of fuel composition by gamma-ray spectroscopy would be ideal for influencing the inserted mix, as a blend of used LWR fuel and reactor-grade plutonium acts as the fissile material for the reactor. When the refueling process is ongoing, removed fission products must be replaced with more fuel blend, and the ability to adjust the ratio between the two fuel types in the inserted blend should be based on current reactor contents. A fuel management loop will allow fuel to be forcibly circulated, the piping passing by a shielded HPGe, and past a series of valves that may allow for total core draining, or for fuel salt to be gradually removed or added.

5.2. Salt at different burnup points

When estimating gammas and masses present in molten salt reactors, assumptions will vary depending on the reactor type. As a somewhat special case, the USSR has its own set of assumptions, as it is a stationary salt reactor intended for waste burning. An isothermal, homogenous fuel composition throughout the reactor is assumed at any given time. Measurements were performed at 17 timesteps, spread across three days of operation and one day of cooling. This short operation span is to account for the fact the reactor fuel would be replaced much more frequently than in any other reactor type if refueled in batches or would be refueled continuously. The energy spectra are mostly shown between 0.50 and 1.00 MeV energies, as this region tends to contain a large number of gamma peaks from fission products and actinides of interest. The initial fueling already contains many actinides as a significant portion of the fuel is from used LWR fuel. Because the only radionuclides present at first are long-lived actinides, many gamma peaks are present, although none are significant.

Fig. 11 shows the initial gamma spectrum along with the spectra from 36 min (0.025 days) later, both ranging from 0.00 MeV to 1.00 MeV. The initial spectrum shows only Uranium (^{234}U, ^{235}U, ^{236}U and ^{238}U), Neptunium (^{237}Np), Plutonium (^{238}Pu, ^{239}Pu, ^{240}Pu, ^{241}Pu and ^{242}Pu), Americium (^{241}Am, ^{242}Am and ^{243}Am) and Curium (^{242}Cm, ^{243}Cm, ^{244}Cm and ^{245}Cm). Like the pebble model, this does not account for metastable radionuclides or decay products. After just 36 min, numerous fission products have been created. The differences in the fuel spectra are significant, as the small peaks indicating the various actinides are obscured by the much larger peaks of their fission products. After only a single burn step, only the fission products directly created by the fuel are visible, although secondary and tertiary fission products are less significant.

Gamma spectra for 0.025, 0.075, 1.050 and 3.000 days of burnup are shown in Fig. 12. These peaks are due primarily to 15 nuclides, shown in Table 1.

Unlike PBRs and most MSRs, the USSR has an initial fuel mix that contains spent fuel, and without replacement, the fuel mix goes subcritical following approximately 4 days of burnup, at which time there is no appreciable buildup of ^{137}Cs, ^{134}Cs or ^{154}Eu. Fig. 13 shows the gamma spectra at 3.000 days of burnup, and at 1.000 day of cooling. A

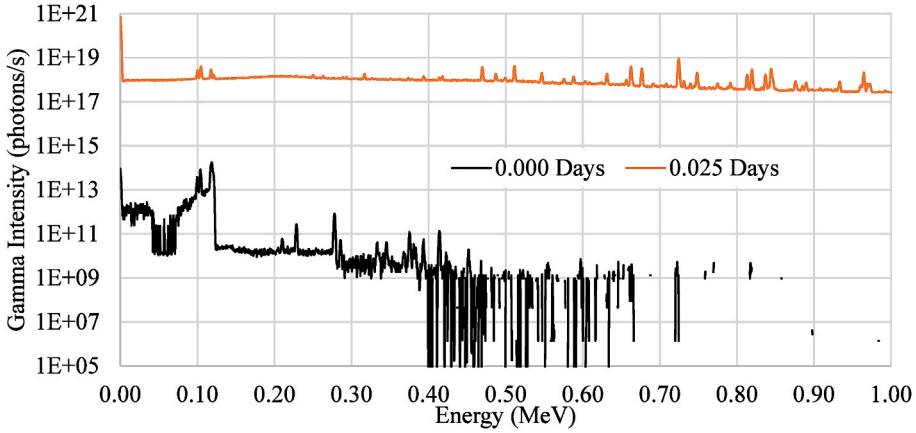

Fig. 11. HPGe gamma spectra of the MSR fuel burned 0.000 and 0.025 days, respectively.

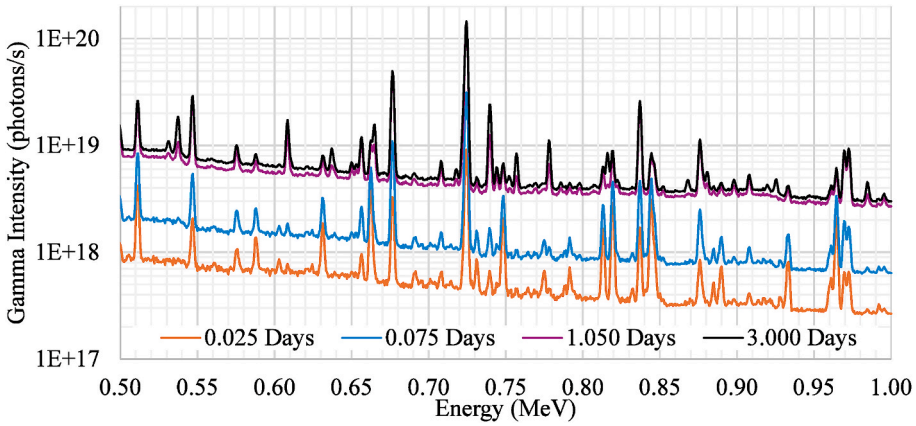

Fig. 12. HPGe gamma spectra of MSR fuel burned 0.025, 0.075, 1.05 and 3 days, respectively.

Table 1
Prominent nuclides with gamma rays emitted between 0.5 MeV and 1.0 MeV.

Nuclide Information			Mass (g) at various timesteps					
Nuclide	$T_{1/2}$ (sec)	Sp. Ac (γ/[g*s])	Initial Loading	Days of burnup at 300MWth				1 Day Cooling
				0.025	0.075	1.05	3	
^{95}Zr	5532365	7.91752E+20	0	0.08792	0.3667	5.897	16.67	16.55
^{99}Mo	237326	5.19548E+21	0	0.1793	0.5523	6.939	15.78	12.27
^{105}Ru	15980	3.76142E+23	0	0.1179	0.4147	1.846	1.894	0.04604
^{131}I	693377	4.92963E+21	0	0.01675	0.17	5.11	14.82	14.66
^{135}I	23688	1.75187E+23	0	0.2562	0.7237	3.903	4.192	0.3334
^{135}Xe	32904	9.45796E+22	0	0.04769	0.2082	4.881	6.991	2.371
^{136}Cs	1124064	8.65551E+21	0	0.004879	0.01465	0.2088	0.7185	0.6817
^{140}Ba	1101686	1.92931E+21	0	0.2306	0.7097	9.751	26.49	25.09
^{140}La	145029	4.46161E+22	0	0.000552	0.002611	0.2602	1.566	2.182
^{143}Ce	118940	3.87504E+22	0	0.1051	0.4782	6.453	12.31	7.505
^{147}Nd	952992	3.35516E+21	0	0.04883	0.2304	3.766	10.01	9.452
^{151}Pm	102240	3.71994E+22	0	0.02135	0.0927	1.162	2.047	1.15
^{239}U	1407.0	9.20596E+23	0	2.238	3.282	3.511	3.665	0
^{238}Np	181354	8.7862E+21	0	0.01429	0.04249	0.498	1.038	0.7483
^{244}Am	36360	1.02947E+23	0	0.004384	0.01264	0.09099	0.1174	0.02261

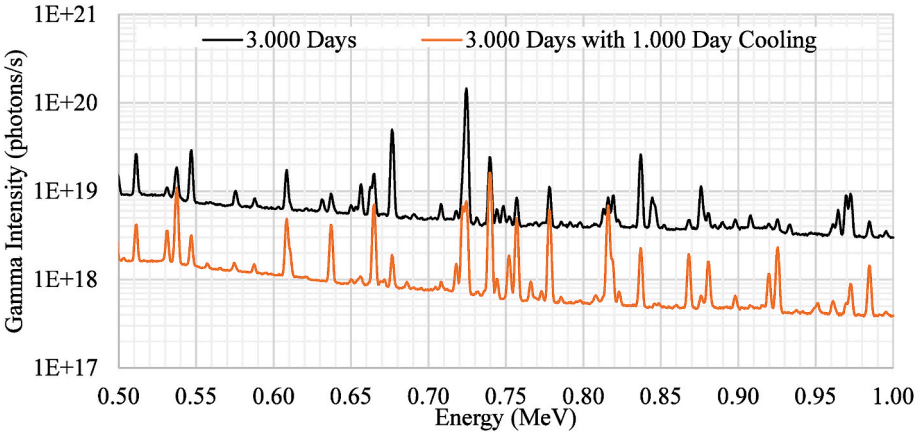

Fig. 13. HPGe gamma spectra of the MSR fuel burned 3.000 days and at 3.000 days of burnup with 1.000 day of cooling.

cooling time of more than a day would be detrimental, as fuel burnup reaching an unsustainable level would no longer be measured by a HPGe system, but by the reactor beginning to power down. Instead, real-time measurements (within a minute of fuel being within the active core) are ideal.

The total spectrum at 3.000 days of burnup is constructed – like others in this work – based on per-nuclide contributions, allowing for it to be deconstructed to show the direct contributions of these 15 nuclides, resulting in Fig. 14. Out of 82 gamma-emitting radionuclides present in the fuel, 67 showed relatively little impact on any specific peaks, with the strongest contribution being ^{38}Cl at 511 keV, contributing only 22.4% of the total gamma intensity in that bin.

Unlike pebble bed reactors, molten salt reactors lack discrete fuel elements. Online refueling takes the form not of removing certain fuel elements and adding fresh ones, but rather a continuous process involving batch reprocessing over timespans varying from hours to

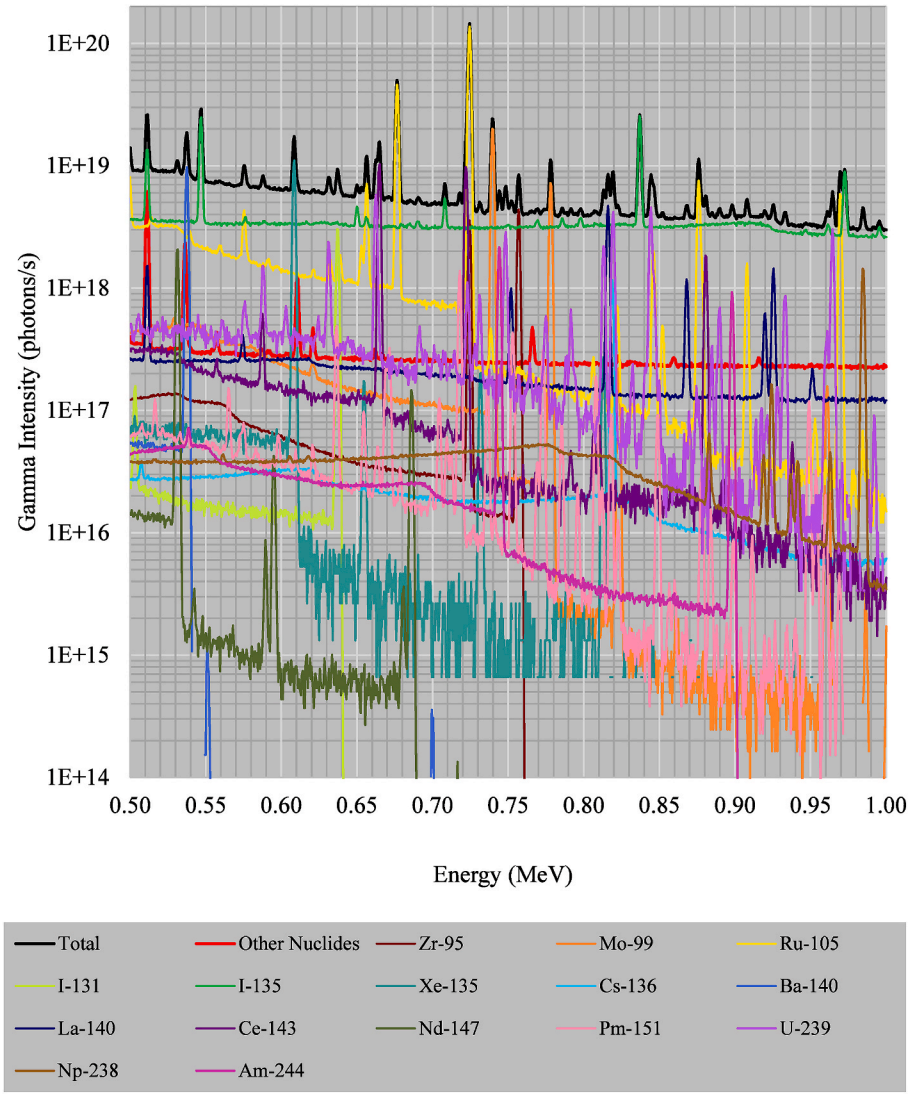

Fig. 14. HPGe total and contributing gamma spectra of the MSR fuel burned for 3.000 days.

weeks to months. While the specifics can vary widely, this process can be used to calculate the approximate fuel composition and level of burnup. This will undoubtedly require careful calibration by comparing readings before, during and after each refueling batch, comparing them to known or computed changes.

Once refined sufficiently, this model can help MSR operators have a better idea of the core composition. The overall magnitude of the gamma continuum serves as a good baseline indication of the core's burnup level and is expected to rise steadily before dropping as one batch is removed and a fresh batch is added, or to remain constant if continual refueling and reprocessing is used instead of batches. Short lived radionuclides such as ^{140}La also can be used to determine recent operating history, as not only are they created by fission, but also the decay of longer-lived fission products. If recent operating history is known, they can instead by used to determine the levels of other radionuclides that may have no gammas or gammas that are not measurable with the detector(s) used. As can be seen in Table 1, ^{140}Ba is the most reliable burnup indicator.

6. Conclusions

This work presents a computational framework for modeling the expected HPGe measured gamma-ray spectrum from known radionuclide inventories. The data presented in this paper results from generating these gamma energy spectra using the known masses of each radionuclide present in the fuel at each stage of burnup and using this mass to scale the results of individual runs that focus on the gamma emissions from each nuclide by itself. The individual runs use average masses in the input decks to account for attenuation, leading to some error, but allowing the same set of runs to be applied with different fuel contents. The envisioned usage of this tool is not limited to using known material compositions to generate a gamma spectrum, but to eventually be used as a part of a broader effort to determine material composition using a measured gamma spectrum. Applying this to a measured gamma spectrum would involve setting each radionuclide's mass and then iterating by adjusting these values to better fit the generated and measured spectra, with the final set of masses being an initial guess. To improve this best fit, a second round of iterations can be performed after running a batch of individual radionuclide tallies using the material masses calculated in the initial guess instead of from the average burnup composition.

MSRs and PBRs are advanced reactors with distinct fuel circulation features, lacking fuel elements which are both stationary and discrete. These same features allow for gamma-spectroscopy measurement of the fuel volume or elements within a minute of the fuel exiting the core. Rather than allowing the fuel to cool for a significant period before taking any measurements, this work assumes an HPGe detector is

incorporated into the fuel circulation loop, allowing for measurement of fuel before short-lived fission products can decay. There are multiple challenges introduced by the distinct fuel circulation features of the MSRs and PBRs. Burnup estimation is one, as the fuel lacks a stationary position in the core, and can often take either circuitous routes or a very direct path, making conventional burnup calculation -using core position and reactor history-unreliable. Nuclear safeguards are another challenge, and although the challenges posed by PBRs and MSRs to nuclear safeguards are different, a tool capable of iteratively determining the material composition of a material based on a measured gamma spectrum would benefit each.

This tool is still in development and has yet to be fully tested and refined. All presented composite plots excluding those of fresh fuel have at most 5.35% uncertainty, with averages of 1.6925% and 2.4928% from 0 MeV to 1 MeV for the pebble and salt models respectively. Composite plots of fresh fuel and individual plots are skewed as some bins receive a single count, with 100% uncertainty. Only 1 billion particles were simulated for each nuclide, as this is a proof of concept.

Future work will involve performing multiple triple comparisons, where a known material composition and fuel form factor are used to generate a pseudo-measured gamma spectrum. The tool presented in this work will be used to generate two gamma spectra, the first, using the known material composition, and the second by iterating the average burnup material composition until the resulting gamma spectrum best matches the pseudo-measured gamma spectrum. Each comparison in the triple comparison yields useful data. Pairing the pseudo-measured and the known composition spectra accounts for the difference in attenuation between the correct composition and the average composition the tool uses for its initial guess. Comparing the two gamma spectra generated by the tool will reveal similarities and differences resulting in using the tool to match the pseudo-measured spectrum or the corresponding material composition. Finally, the third comparison compares the pseudo-measured spectrum and correct material composition with a gamma spectrum and material composition iteratively calculated to match the measurement.

CRediT authorship contribution statement

Justin Shurie: Data curation, Formal analysis, Investigation, Methodology, Validation, Visualization, Writing – original draft. **Ben Impson:** Data curation, Formal analysis, Investigation, Methodology, Validation, Visualization, Writing – review & editing. **Zeyun Wu:** Conceptualization, Funding acquisition, Investigation, Project administration, Supervision, Writing – review & editing. **Braden Goddard:** Conceptualization, Funding acquisition, Investigation, Methodology, Project administration, Resources, Supervision, Writing – review & editing.

Declaration of competing interest

The authors declare the following financial interests/personal relationships which may be considered as potential competing interests: All authors report financial support, equipment, and/or supplies, and travel were provided by Virginia Commonwealth University. All authors report financial support and/or travel were provided by US Department of Energy.

Acknowledgements

This work is performed with the support of the U.S. Department of Energy's (DOE) Nuclear Energy University Program (NEUP) with the Award No. DE-NE0009304 and No. DE-NE009421. The authors acknowledge the College of Engineering at the Virginia Commonwealth University for providing high-performance computing resources that have contributed to the research results reported within this paper. The first author was also supported under the DOE NEUP Graduate Fellowship. Any opinions, findings, conclusions or recommendations expressed in this publication are those of the author(s) and do not necessarily reflect the views of the DOE Office of Nuclear Energy.

Data availability

Data will be made available on request.

References

Bolzonella, M., 2023. Benefits and drawbacks of non-destructive assay (NDA) for nuclear safeguards – an overview. IJNSNP 65, 63–73. https://doi.org/10.3011/ESARDA.IJNSNP.2023.6.

Carter, A., Lange, T., Balestra, P., Strydom, G., Sen, S., Wang, R., 2022. XE-100 modeling and simulation for neutronic analysis in MCNP6.2. In: *Proceedings of the International Conference on Physics of Reactors, PHYSOR 2022*. Proceedings of the International Conference on Physics of Reactors, PHYSOR 2022. American Nuclear Society, pp. 58–67. https://doi.org/10.13182/PHYSOR22-37642.

Caruso, S., Murphy, M., Jatuff, F., Chawla, R., 2007. Validation of 134Cs, 137Cs and 154Eu single ratios as burnup monitors for ultra-high burnup UO2 fuel. Ann. Nucl. Energy 34 (1), 28–35. https://doi.org/10.1016/j.anucene.2006.11.009.

Claxton, K.T., 1966. A review of pebble bed reactors and the characteristics of packed beds. J. Nucl. Energy - Parts A/B React. Sci. Technol. 20 (9), 735–777. https://doi.org/10.1016/0368-3230(66)90157-1.

Dim, O., Hu, J., Hartanto, D., Cui, Y., Soto, C., Gibbs, P., 2023. Modeling and Simulation of Fuel Burnup in Pebble Bed Reactors. Oak Ridge National Laboratory (ORNL), Oak Ridge, TN (United States). https://www.osti.gov/biblio/1986214.

Dragnev, T., 1973. Non-destructive assay techniques for nuclear safeguards measurements. Atom. Energy Rev. 11 (2), 341–368.

From ENSDF database as of March 7th. Version available at: http://www.nndc.bnl.gov/ensarchivals/.

Gawad, K.A.E., Zhang, Z., Song, Y., Zahraddeen, A., Hazzaa, M.H., 2019. Study on the performance of some non-destructive methods to estimate the uranium enrichment in nuclear materials. Results Phys. 13, 102345. https://doi.org/10.1016/j.rinp.2019.102345.

Geist, W.H., Santi, P.A., Swinhoe, M.T., 2024. Nondestructive Assay of Nuclear Materials for Safeguards and Security, second ed. Springer, Cham. https://doi.org/10.1007/978-3-031-58277-6.

Impson, B., Elhareef, M., Wu, Z., Goddard, B., 2025. Influence of TRISO fuel particle arrangements on pebble neutronics and isotopic evolution. J. Nuclear Eng. 6. https://doi.org/10.3390/jne6030027.

International Atomic Energy Agency (IAEA), 2024. ENDSDF, fields=decay_rads&nuclides="/all nuclides/"&rad_types=g. March 7th.

Kovacic, D.N., Gibbs, P., Hu, J., et al., 2023. Nuclear Material Control & Accounting for Pebble Bed Reactors (FY 2023 Summary Report). https://doi.org/10.2172/2434394.

Kovacic, D.N., Worrall, A., Evans, L.G., et al., 2018. Safeguards Challenges for Molten Salt Reactors. Oak Ridge National Laboratory (ORNL), Oak Ridge, TN (United States). https://www.osti.gov/biblio/1474868.

Lakosi, L., Veres, Á., 1990. Nondestructive assay of fission products in spent-fuel assemblies using gamma and photoneutron activation. Nucl. Instrum. Methods Phys. Res. Sect. A Accel. Spectrom. Detect. Assoc. Equip. 299 (1), 463–467. https://doi.org/10.1016/0168-9002(90)90826-R.

Loza P. X-Energy, LLC, submittal of Xe-100 topical report: TRISO-X pebble fuel qualification methodology, revision 2. Published online September 2, 2021. https://www.nrc.gov/docs/ML2124/ML21246A289.pdf.

Mehta, K.S., Goddard, B., Wu, Z., 2024. Neutronics analysis on high-temperature gas-cooled pebble bed reactors by coupling Monte Carlo method and discrete element method. Energies 17 (20). https://doi.org/10.3390/en17205188.

Mulyana, D., Chirayath, S.S., 2024. A gamma spectroscopy-based non-destructive approach for pebble bed reactor safeguards. Ann. Nucl. Energy 195, 110186. https://doi.org/10.1016/j.anucene.2023.110186.

Reinovsky, R.E., Favalli, A., 2019. TECHNIQUES AND TECHNOLOGY OF NON-DESTRUCTIVE ANALYSIS FOR NUCLEAR MATERIALS SECURITY. Los Alamos National Laboratory (LANL). https://www.osti.gov/biblio/1508536.

Serp, J., Allibert, M., Beneš, O., et al., 2014. The molten salt reactor (MSR) in generation IV: overview and perspectives. Prog. Nucl. Energy 77, 308–319. https://doi.org/10.1016/j.pnucene.2014.02.014.

Shurie, J., Krushelnisky, R., King, C., Strom, W., Wu, Z., 2024. A Novel Stationary Molten Salt Reactor Design for Spent Nuclear Fuel Burning. American Nuclear Society. https://www.ans.org/meetings/student2024/session/view-2444/.

Snook, R.L., 2024. Modeling the Radiation Shielding Effectiveness of Hafnium Diboride Reinforced Epoxy Composites Using MCNP. Master's Thesis. Virginia Commonwealth University. https://scholarscompass.vcu.edu/etd/7794.

Snook, R., Erdogan, F., Rojas, J., Goddard, B., 2026. Radiation shielding effectiveness of hafnium diboride-epoxy composites using MCNP simulation. Radiat. Phys. Chem. 239, 113277. https://doi.org/10.1016/j.radphyschem.2025.113277.

Status of Molten Salt Reactor Technology, 2023. INTERNATIONAL ATOMIC ENERGY AGENCY. https://www.iaea.org/publications/14998/status-of-molten-salt-reactor-technology.

Suparlina, L., Setiadipura, T., 2019. Suwoto. Burnup calculation study of pebble bed equilibrium core. J. Phys., Conf. Ser. 1198 (2), 022036. https://doi.org/10.1088/1742-6596/1198/2/022036.

Turinsky, P.J., Keller, P.M., Abdel-Khalik, H.S., 2005. Evolution of nuclear fuel management and reactor operational aid tools. Nucl. Eng. Technol. 37 (1), 79.
Werner, C.J., Bull, J.S., Solomon, C.J., et al., 2018. MCNP Version 6.2 Release Notes. Los Alamos National Lab. (LANL), Los Alamos, NM (United States). https://doi.org/10.2172/1419730.
Willman, C., Håkansson, A., Osifo, O., Bäcklin, A., Svärd, S.J., 2006. Nondestructive assay of spent nuclear fuel with gamma-ray spectroscopy. Ann. Nucl. Energy 33 (5), 427–438. https://doi.org/10.1016/j.anucene.2005.12.005.
Zafar, Z.I., Park, Y.S., Kim, M.H., 2019. Evaluation of the reutilization of used nuclear fuel in a PWR core without reprocessing. Nucl. Eng. Technol. 51 (2), 345–355. https://doi.org/10.1016/j.net.2018.09.026.